Pharmacological Research 107 (2016) 282–290

Contents lists available at ScienceDirect

Pharmacological Research

journal homepage: www.elsevier.com/locate/yphrs

The water soluble ruthenium(II) organometallic compound [Ru(*p*-cymene)(bis(3,5 dimethylpyrazol-1-yl)methane)Cl]Cl suppresses triple negative breast cancer growth by inhibiting tumor infiltration of regulatory T cells

Maura Montani[a,1], Gretta V. Badillo Pazmay[a,b,1], Albana Hysi[c,1], Giulio Lupidi[b,**], Riccardo Pettinari[b], Valentina Gambini[a], Martina Tilio[a], Fabio Marchetti[d], Claudio Pettinari[b], Stefano Ferraro[d], Manuela Iezzi[c], Cristina Marchini[a], Augusto Amici[a,*]

[a] School of Bioscience and Veterinary Medicine, University of Camerino, Camerino, MC, 62032, Italy
[b] School of Pharmacy, University of Camerino, Camerino, MC, 62032, Italy
[c] Aging Research Centre, G. d'Annunzio University, Chieti, 66100, Italy
[d] School of Science and Technology, University of Camerino, Camerino, MC, 62032, Italy

ARTICLE INFO

Article history:
Received 21 September 2015
Received in revised form 11 February 2016
Accepted 1 March 2016
Available online 30 March 2016

Keywords:
Ruthenium(II)
Organometallic arene complexes
Anticancer drugs
Triple negative breast cancer
In vivo tests
Tumor infiltrating regulatory T cells

ABSTRACT

Ruthenium compounds have become promising alternatives to platinum drugs by displaying specific activities against different cancers and favorable toxicity and clearance properties. Here, we show that the ruthenium(II) complex [Ru(*p*-cymene)(bis(3,5-dimethylpyrazol-1-yl)methane)Cl]Cl (UNICAM-1) exhibits potent *in vivo* antitumor effects. When administered as four-dose course, by repeating a single dose (52.4 mg kg-1) every three days, UNICAM-1 significantly reduces the growth of A17 triple negative breast cancer cells transplanted into FVB syngeneic mice. Pharmacokinetic studies indicate that UNICAM-1 is rapidly eliminated from kidney, liver and bloodstream thanks to its high hydrosolubility, exerting excellent therapeutic activity with minimal side effects. Immunohistological analysis revealed that the efficacy of UNICAM-1, mainly relies on its capacity to reverse tumor-associated immune suppression by significantly reducing the number of tumor-infiltrating regulatory T cells. Therefore, UNICAM-1 appears very promising for the treatment of TNBC.

1. Introduction

Breast cancer is a heterogeneous disease classified into molecular subtypes with distinctive gene expression signatures. Of all the molecular subtypes, triple negative breast cancer (TNBC) has the worst negative outcome and prognosis [1,2]. TNBCs occur most frequently in young women and tend to exhibit aggressive metastatic behavior [3]. TNBCs are estrogen receptor (ER) and progesterone receptor (PR)-negative and also lack high expression/amplification of HER2, limiting targeted therapeutic options [4]. New therapies against this breast cancer subtype are therefore an urgent unmet medical need. Cisplatin (*cis*-[PtIICl2(NH3)2]) is well established as an effective drug for the treatment of testicular cancer and, in combination with other chemotherapeutic agents, for ovarian, cervical, brain, bladder, lung, and breast cancers [5,6]. Recently, preclinical and clinical data have revealed encouraging anticancer activity of cisplatin as single-agent in patients with TNBC [7,8]. Despite the success of platinum-based drugs, their continued use is greatly limited by severe dose limiting side effects and intrinsic or acquired drug resistance [9–11]. In the search for anticancer agents containing nobel metals other than platinum, ruthenium compounds have turned out to be a cutting-edge class of anticancer compounds [12–18]. Accordingly, two ruthenium(III)-based compounds, namely

* Corresponding author at: School of Bioscience and Veterinary Medicine, via Gentile III Da Varano, University of Camerino, Camerino, 62032, Italy.
** Corresponding author.
E-mail addresses: giulio.lupidi@unicam.it (G. Lupidi), augusto.amici@unicam.it (A. Amici).
[1] These authors contributed equally to this work.

http://dx.doi.org/10.1016/j.phrs.2016.03.032
1043-6618/

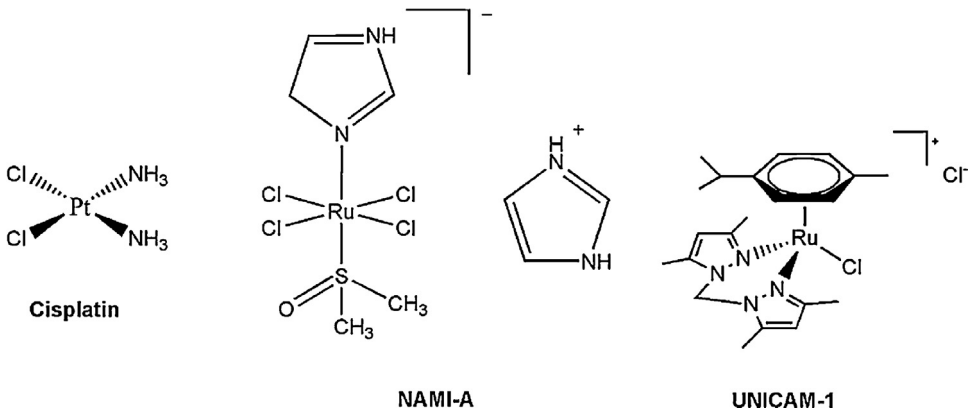

Fig. 1. Chemical structures of cisplatin, NAMI-A and UNICAM-1.

NAMI-A (imidazolium *trans*-[tetrachloro(dimethylsulfoxide)(1H-imidazole)ruthenate(III)]) [19] and NKP1339 sodium *trans*-[tetrachloridobis(1Hindazole)ruthenate(III)] [20], are currently ongoing in phase II clinical trials. The different toxicity profiles between platinum- and ruthenium-based compounds could probably due to different targets. It is widely accepted that the antineoplastic properties of platinum compounds rely on their interaction with DNA, which, in turn, activates cell death [21]. Instead, the mechanisms by which ruthenium-based drugs exert their anticancer effects remain to be fully elucidated but recent evidence suggests that ruthenium compounds are most likely to be multitargeted [22,23]. Thus, they could represent a valid therapeutic alternative to platinum-based drugs which are often associated with an unfavorable toxicity profile. Among the ruthenium(II) organometallic complexes, the half sandwich arene–ruthenium subgroup, in particular, offers a great promise in the field of cancer therapy. Two prototypical compounds reported by Aird et al. [24] and RAPTA-C developed by Scolaro et al. [25] have shown relevant therapeutic potential. We have recently reported an extensive study on the coordination chemistry of ruthenium arene fragments with bis(pyrazol-1-yl)methan ligands [26]. In this work we extend our investigation to the *in vivo* antitumor activity of the prototype compound, [Ru(*p*-cymene)(bis(3,5-dimethylpyrazol-1-yl)methane)Cl]Cl, termed UNICAM-1 (Fig. 1). The results presented here reveal that UNICAM-1 has significant anticancer activity in a murine model of TNBC and results to be well tolerated, showing considerably reduced side-effects when compared to cisplatin and NAMI-A. The analysis of tumor immune infiltrate suggests that the response to this new chemotherapeutic agent relies mainly on its capacity to elicit an anticancer immunosurveillance.

2. Material and methods

2.1. Compounds

NAMI-A was prepared according to a patented procedure [27]. Cisplatin was obtained by Sigma Chemical Co. (St. Louis, MO). UNICAM-1 was prepared as previously described [26] and its analytical and spectroscopic data have been reported in the Supplementary materials.

2.2. Cell cultures, cell proliferation assay and lysates preparation

A17 cells were established from spontaneous lobular carcinomas that arose in a FVB/neuT mice transgenic for the activated isoform of rat HER-2/neu oncogene (FVB/neuT233), as previously described [28,29]. A17 cells were cultured in Dulbecco's Modified Eagle Medium (DMEM, Invitrogen, Carlsbad, CA) supplemented with 20% fetal bovine serum (FBS, Invitrogen, Carlsbad, CA) and 1% penicillin–streptomycin (Invitrogen, Carlsbad, CA). Human breast cancer MDA-MB 231 cells were obtained from American Type Culture Collection (Rockville, MD) and cultured in DMEM supplemented with 10% FBS and 1% penicillin-streptomycin. Cells were grown in a humidified atmosphere with 5% CO_2 at 37 °C. UNICAM-1 effect on cell viability, respect to cisplatin and NAMI-A, was evaluated by seeding 2.5×10^3 cells/well (A17 cells) or 7×10^3 cells/well (MDA-MB-231 cells) in octuplicate in 96 well plates in complete medium. The day after, fresh medium containing appropriate concentrations of UNICAM-1, NAMI-A and cisplatin (all dissolved in isotonic solution, 0.9% $NaCl_{(aq)}$) were added. After 72 h cell viability was determined using an MTT (Sigma Aldrich, St. Louis, MO) assay, as previously described [30]. The cytotoxicity of the compounds was reported as percentage of viable cells relative to control cells. All the experiments were repeated three times. For cell lysates preparation, 4×10^5 cells/well (A17 cells) or 8×10^5 cells/well (MDA-MB-231 cells) were seeded in 6-well plates, treated with UNICAM-1, NAMI-A and cisplatin drugs for 48 h, harvested, and lysed in RIPA buffer (1% NP40, 0.5% Na-deoxycolic acid and 0.1% SDS in PBS) with fresh protease inhibitors (Protease Inhibitor Cocktail, Sigma Aldrich, St. Louis, MO).

2.3. Animals

Female FVB/NCrl mice were obtained from Charles River S.r.l. (Lecco, Italy), and housed under controlled conditions. Mice were treated according to the European Community guidelines. The Animal Research Committee of the University of Camerino authorized the experimental protocol.

2.4. Treatments and tumor growth

10^5 A17 cells were inoculated in 200 μl of PBS into mammary fat pad of 8-week-old FVB females. 10 days after tumor challenge, mice were randomly divided in 4 groups (10 mice per group) and treated with UNICAM-1, NAMI-A, cisplatin or isotonic solution (vehicle) by intraperitoneal injection (*via* i.p) in accordance with two different dosage and treatment schedules (protocol q3 × 4 or q1 × 6) as previously reported [31]. According to protocol q1 × 6, 35 mg/kg/day of ruthenium complexes (210 mg/kg/day final amount) and 2 mg/kg/day of cisplatin (12 mg/kg/day final amount) were administered for six consecutive days. According to protocol q3 × 4, 52.5 mg/kg/day of ruthenium complexes (210 mg/kg/day final amount), and 3 mg/kg/day of cisplatin (12 mg/kg/day final amount) were administered four times, once every three days. Body weight of mice receiving UNICAM-1, NAMI-A and cisplatin was checked once a week and compared with untreated controls. Tumor

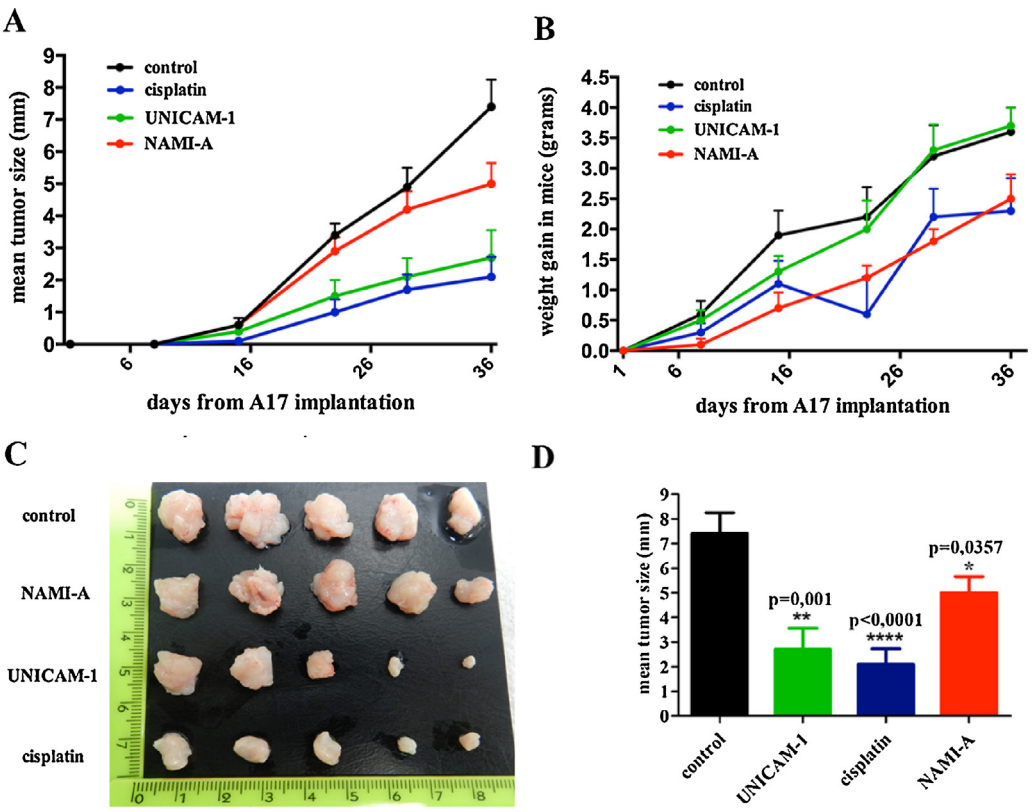

Fig. 2. UNICAM-1 suppressed TNBC growth *in vivo*. FVB female mice were injected with syngeneic A17 cells (10^5). Mice were treated with UNICAM-1, cisplatin, NAMI-A or isotonic solution. Treatments (q3 × 4 schedule) started ten days after cell injections. (A) Tumor growth curves in mice receiving q3 × 4 treatment schedule. Values are mean ± SEM, n = 10. (B) Effect of treatments on mean body weight of mice. Values are mean ± SEM. (C) Images of representative tumors explanted from control and treated mice 36 days after tumor challenge. (D) Average tumor diameter in treated *vs* control mice at day 36. Values are mean ± SEM, n = 10. *p < 0.05; **p < 0.01; ***p < 0.001; ****p < 0.0001 was calculated with an unpaired two-tailed *t* test. Each group was compared to control.

growth was checked once a week using an electronic caliper until the end of the experiment. Tumors were surgically removed on day 39, in the q1 × 6 protocol, or day 36, in the q3 × 4 protocol.

2.5. Histology and immunohistochemistry

Tumors, kidneys and livers were harvested at the end of the experimental period, fixed in formalin and embedded in paraffin or fixed in PFA 4% and frozen in cryo-embedding medium (OCT Bioptica, Milan, Italy). To detect possible organ toxicity, kidney and liver slides were stained with hematoxylin and eosin. Histopathological evidences of acute tissue damage were semi-quantified according to the methodology described elsewhere [32]. For each organ, two slides were analyzed in a blind fashion evaluating the following parameters: central vein congestion, inflammatory aggregate, focal hepatic necrosis, dilated sinusoids, breakdown hepatocytes, perivascular inflammatory aggregate, degenerated hepatic cord, apoptotic cells, vacuolations for liver sections and atrophic glomerulus, dilated proximal convoluted tubule, degenerated tubules, inflammatory cells infiltrate, desquamation of epithelial cells and cast formation for kidney sections. The severity and incidence of each parameter was scored as follows: grade 0 = absent; grade 1 = mild; grade 2 = moderate; grade 3 = severe. For immunohistochemistry tumor slides were incubated with the following primary antibodies: rabbit mAb anti-cleaved caspase-3 (MAB835, R&D Systems, Milan, Italy), rat mAb anti-CD4 (550278), anti-CD8α (550281), anti-CD11b (550282), anti-CD45R/B220 (550286), anti-CD31 (550274), anti-CD105 (550546), anti-Gr-1(550291), (all from BD Pharmingen, Milan, Italy); anti-CD68 (ab53444 Abcam, Cambridge, UK) and anti-Foxp3 (14-5773, eBioscience, Milan, Italy); after washing, slides were overlaid with appropriate secondary antibodies. Immunostaining was developed with DAB Chromogen System (Dako, Milan, Italy) or Vulcan Fast Red (Biocare, Milan, Italy) alkaline phosphatase method. The number of cleaved caspase-3 positive cells and CD31/105 positive vessels was evaluated on digital images of controls, cisplatin, NAMI-A and UNICAM-1 tumors (10 per group, 5 × 400 microscopic fields per tumor).

2.6. Metal trace examination

Ruthenium and platinum content in explanted livers and kidneys from mice treated with UNICAM-1, NAMI-A, cisplatin or isotonic solution were evaluated by Inductively Coupled Plasma-Mass Spectrometry (ICP-MS). Metal content in sera of mice were measured at 7, 14, 30 and 60 days from the beginning of the treatments. All solutions were prepared using ultrapure water obtained from a Millipore Milli-Q system (resistivity 18.2 MΩ cm). Optimized digestion of samples (Supplementary Table I) was carried out in a microwave digestor (Berghof Speedwave four, Berghof, Eningen, Germany) with 5 ml of HNO_3 (65%). Fifty microliters of iridium solution (20 mg) was added as recovery standard. Digested solutions were diluted with ultrapure water to obtain a solution with the correct acid concentration in order to perform analysis. The concentrations of ruthenium in the processed samples were measured by ICP-MS (7500cx series) with the operating conditions described elsewhere [33]. Calibration curves were obtained using aqueous standard solutions (1.5% nitric acid) with appropriate stock standards dilutions (Fluka Analytical, Aldrich, Milan, Italy).

Table 1
Half Maximal Inhibitory concentration (IC_{50}) values were calculated for A17 and MDA-MB231 cells treated for 72 h with increasing concentrations of tested compounds.

	IC_{50} (μM) ± SD		
	Cisplatin	NAMI-A	UNICAM-1
A17	6.93 ± 0.14	485.58 ± 0.02	230.66 ± 0.02
MDA-MB 231	38.70 ± 0.03	840.21 ± 0.03	409.89 ± 0.04

2.7. Immunoblotting analysis

Tumor lysates were obtained as previously described for cell lysates preparation. Lysates (40 μg/lane) were separated by 4–20% gradient precast SDS-PAGE (Bio-Rad) and transferred onto polyvinylidene difluoride (PVDF) membranes (Immobilon P, Millipore). Rabbit monoclonal antibodies against COX2 and cleaved caspase-3 and rabbit polyclonal antibody against caspase-3 were from Cell Signaling (Beverly, MA, USA). Secondary antibody conjugated with peroxidase was from Sigma–Aldrich (St. Louis, MO, USA). The immunoreactive bands were detected by using LiteAblot PLUS (Euroclone) detecting reagents and pictures were acquired with ChemiDoc Imaging System (Bio-Rad).

2.8. Statistical analysis

Quantitative data are presented as means ± SEM from at least three independent experiments. The significance of differences was evaluated with two-tailed Students *t*-test, or one way ANOVA followed by Bonferroni post test. Statistical analysis was carried out with GraphPad Prism5 Software (San Diego, CA, USA). $p \leq 0.05$ was used as the critical level of significance.

3. Results and discussion

3.1. *UNICAM-1 inhibited TNBC growth* in vitro

The effect of UNICAM-1, compared with that of NAMI-A and cisplatin, on cancer cell viability was estimated by MTT assay at 72 h treatment using the human MDA-MB-231 cells and the murine A17 cells as models of TNBC. A17 cells were established from an FVB/neuT transgenic mammary tumor and were previously described as strongly related to TNBC [34]. Although the ruthenium(II) complexes showed a lower effectiveness respect to cisplatin, they are able to inhibit viability of both cell lines in a dose-dependent manner, where UNICAM-1 proved more efficient than NAMI-A as reported in Table 1 and Supplementary Fig. 1. We next studied whether these inhibitory effects of ruthenium(II) complexes on cells viability were the result of apoptosis. Interestingly, only UNICAM-1 resulted in the induction of cell death by the activation of the apoptotic "executioner" caspase-3 (Supplementary Fig. 2) when compared to NAMI-A or cisplatin treatments. Taken together, these results suggest that UNICAM-1 leads to apoptosis of TNBC cells, showing promising *in vitro* anticancer activity.

3.2. *UNICAM-1 inhibited TNBC growth* in vivo

We next investigated the *in vivo* antineoplastic effects of UNICAM-1 against A17 cells, able to give rise to aggressive mesenchymal tumors when injected into syngeneic mice. A17 cells share molecular signature with TNBC, including expression of vimentin, cytokeratin 14, and *N*-cadherin as we previously described [28,34]. A key feature of A17-signature is also the overexpression of COX2, a mesenchymal hallmark in tumors, whose relevance in growth, vasculogenesis and invasiveness has been widely documented in various types of carcinoma, both in clinical and experimental studies [35,36]. Here we have shown that UNICAM-1 is able to significantly reduce A17 transplantable tumors growth in FVB syngeneic mice (Fig. 2). The efficacy of UNICAM-1 as antitumoral agent was compared with that of cisplatin and NAMI-A. In an attempt to optimize a treatment schedule, resulting in a powerful anticancer action associated with minimal side-effects, the same final concentration of UNICAM-1 (210 mg/kg) or cisplatin (12 mg/kg) or NAMI-A (210 mg/kg) was administered according to two different protocols: a) treatment called q1 × 6 (intraperitoneal (i.p.) injection of UNICAM-1 (35 mg/kg/day) or cisplatin (2 mg/kg/day) or NAMI-A (35 mg/kg/day), repeated for 6 consecutive days); b) treatment called q3 × 4 (i.p. injection of UNICAM-1 (52.5 mg/kg/day) or cisplatin (3 mg/kg/day) or NAMI-A (52.5 mg/kg/day), repeated 4 times at intervals of 3 days). Although both protocols were effective (Supplementary Fig. 3), tumor growth inhibition became more significant in q3 × 4 treatment, where UNICAM-1 displayed the same anticancer activity of cisplatin (Fig. 2), suggesting that the protocol of administration, not only the dosages, are critical features. Focusing on q3 × 4 drug regimen, it is

Table 2
Semiquantitative analysis of morphological injury parameters in liver and kidney of control, UNICAM-1, cisplatin and NAMI-A groups.

	CONTROLS	UNICAM-1(52.5 mg/Kg)	CISPLATIN(3 mg/Kg)	NAMI-A (52.5 mg/Kg)
Liver				
Central vein congestion (CVC)	0.8333 ± 0.4082	0.3333 ± 0.2582*,***	**1.167 ± 0.7528**	0.5833 ± 0.5845
Inflammatory aggregate (IA)	0.8333 ± 0.4082	0.5833 ± 0.5845$^{\#}$	1.417 ± 0.7360	**1.667 ± 0.9309**
Focal hepatic necrosis (FHN)	0.4167 ± 0.3764	0.6667 ± 0.5164	**0.7500 ± 0.6892**	0.6667 ± 0.4082
Dilated sinusoids (DS)	0.6667 ± 0.4082	0.7500 ± 0.5244	**1.000 ± 0.4472**	0.9167 ± 0.3764
Moderate breakdown hepatocytes (MBH)	0.7500 ± 0.5244	0.4167 ± 0.4916	**1.000 ± 0.6325**	**1.000 ± 0.7071**
Perivascular inflammatory aggregate (PIA)	0.9167 ± 0.5845	0.5000 ± 0.3162$^{***,\#}$	1.417 ± 0.8612	**1.500 ± 0.7071**
Degenerated hepatic cord (DHC)	0.6667 ± 0.2582	1.250 ± 0.2739**	1.250 ± 0.6892	**1.500 ± 0.6325***
Apoptotic cells (AC)	0.0 ± 0.0	0.5000 ± 0.4472*	**1.167 ± 0.6831****	0.3333 ± 0.2582*,***
Vacuolations (V)	0.08333 ± 0.2041	**1.000 ± 1.581**	0.8333 ± 1.211	0.4167 ± 0.8010
Kidney				
Atrophic glomerulus (G)	0.5833 ± 0.3764	1.083 ± 0.2041*	0.7500 ± 0.6892	**1.167 ± 0.6055**
Dilated proximal convoluted tubule (PCT)	0.8333 ± 0.2582	**0.9167 ± 0.3764**	0.7500 ± 0.6892	**0.9167 ± 0.5845**
Degenerated tubules (T)	0.3333 ± 0.2582	0.8333 ± 0.4082*	0.6667 ± 0.4082	**1.250 ± 0.6124****
Inflammatory cells infiltrate (I)	0.5833 ± 1.201	0.3333 ± 0.4082	**0.9167 ± 1.281**	0.08333 ± 0.2041
Desquamation of epithelial cells (D)	0.2500 ± 0.4183	**0.8333 ± 0.4082***	0.7500 ± 0.4183	0.7500 ± 0.8216
Cast formation (C)	0.08333 ± 0.2041	**0.1667 ± 0.2582**	**0.1667 ± 0.2582**	**0.1667 ± 0.2582**

Values are given as mean ± SD. The group with the higher score for each analyzed injury parameter is evidenced by bold character.
* $p < 0.05$ *vs.* Control group.
** $p < 0.01$ *vs.* Control group.
*** $p < 0.05$ *vs.* Cisplatin group.
$^{\#}$ $p < 0.05$ *vs.* NAMI-A group.

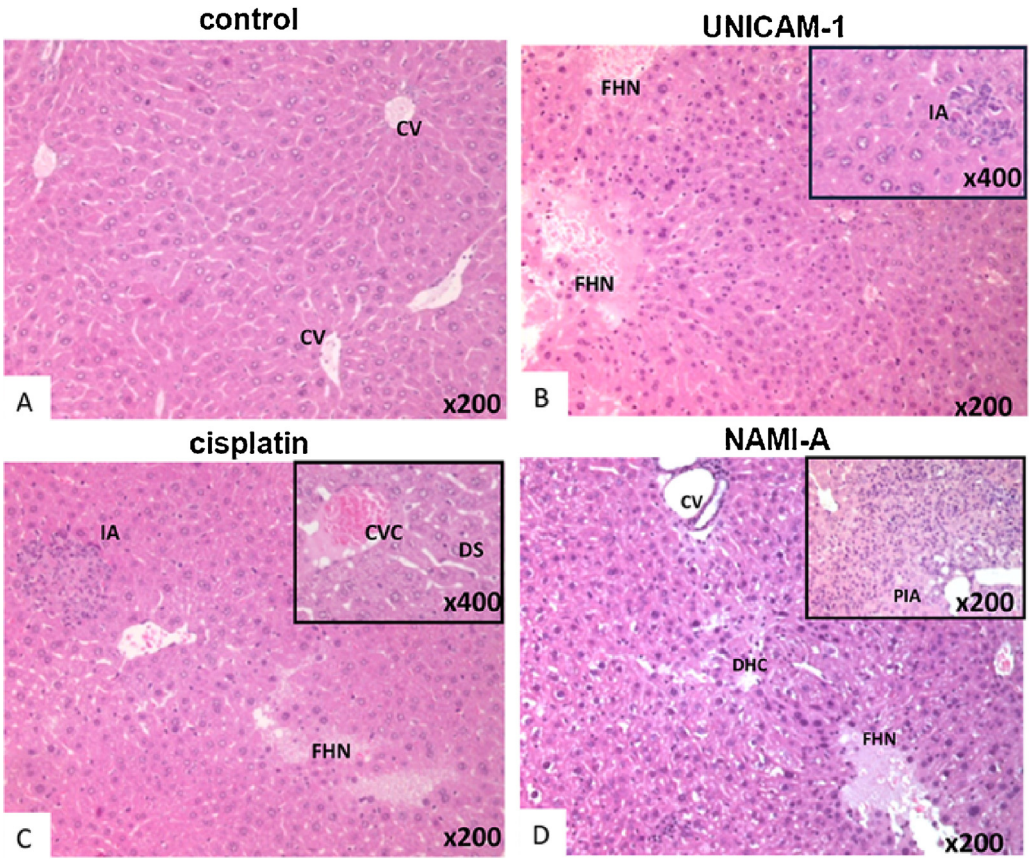

Fig. 3. Histopathological analysis of liver using hematoxylin and eosin (H&E) staining. Representative sections of liver from different treatment groups are shown. CV, central vein; CVC, central vein congestion; IA, inflammatory aggregate; FHN, focal hepatic necrosis; DS, dilated sinusoids; DHC, degenerated hepatic cord; PIA, perivascular inflammatory aggregate.

possible to appreciate how A17 tumor grow rate (Fig. 2A) and the final tumor dimensions (Fig. 2C and D) were significantly reduced in the UNICAM-1- and cisplatin-treated groups compared to the control group, whereas NAMI-A was less effective. While all control mice developed palpable tumors after two weeks from A17 cell challenge, two of the total ten mice treated with UNICAM-1 did not develop palpable tumors until the end of the experiment. Of note, as shown in the tumor growth graph, tumors developed in control mice displayed a rapid growth rate, reaching an average diameter of 7 mm at the end of the study (on day 36 after challenge), whereas tumors developed in the UNICAM-1 treated mice remained very small, with an average diameter never exceeding 3 mm. Interestingly, body weight did not significantly differ between UNICAM-1-treated and control mice (Fig. 2B), suggesting the absence of drug toxicity at the selected dose level. On the contrary, both NAMI-A- and cisplatin-treatments were associated with weigh loss (Fig. 2B).

3.3. UNICAM-1 exhibited markedly reduced liver toxicity compared to cisplatin

An extensive histopathological analysis with the evaluation of several tissue injury parameters was carried out on explanted liver and kidney, common targets of chemotherapy drugs toxicity. Table 2 shows moderate kidney toxicity levels similar for the three drugs, except for the presence of inflammatory cells infiltrate only in cisplatin treated kidneys. Importantly, liver toxicity was much less evident in UNICAM-1 than in cisplatin or NAMI-A treated mice (Table 2 and Fig. 3). Pharmacokinetic studies indicated that UNICAM-1 was rapidly lost from the organs and the bloodstream thanks to its high hydrosolubility, in agreement with lack of serious side effects. In particular, analysis of traces of ruthenium and platinum in the livers and kidneys of treated mice clearly demonstrated a high elimination of UNICAM-1. In contrast, repeated administrations of NAMI-A and cisplatin lead to an accumulation of ruthenium and platinum respectively, preferentially in the kidneys (Fig. 4A). Moreover, blood analysis demonstrated that ruthenium and platinum were still circulating seven days after the last administration of NAMI-A and cisplatin, whereas ruthenium traces were almost undetectable one week after the last UNICAM-1 treatment (Fig. 4B).

3.4. UNICAM-1 impaired tumor angiogenesis and induced apoptosis in TNBC

Histological and immunohistochemical analyses carried out on explanted tumors showed several differences among control and treated mice. Notably, while all three treatments provoke a reduction in the number of vessels, a significantly increased number of apoptotic cells (cleaved caspase-3 positive cells) was visible only in UNICAM-1 treated tumors (Fig. 5), suggesting that the inhibitory activity of UNICAM-1 on tumor growth was due, at least in part, to cell death induction through apoptosis.

3.5. UNICAM-1 suppressed TNBC growth by inhibiting tumor infiltration of regulatory T cells

Chemotherapy seems to be efficient if it succeeds in eliciting anticancer immunosurveillance, that implies the activation of an immune response specific for malignant cells [37]. Antineoplastic agents may stimulate immunosurveillance by acting on cancer

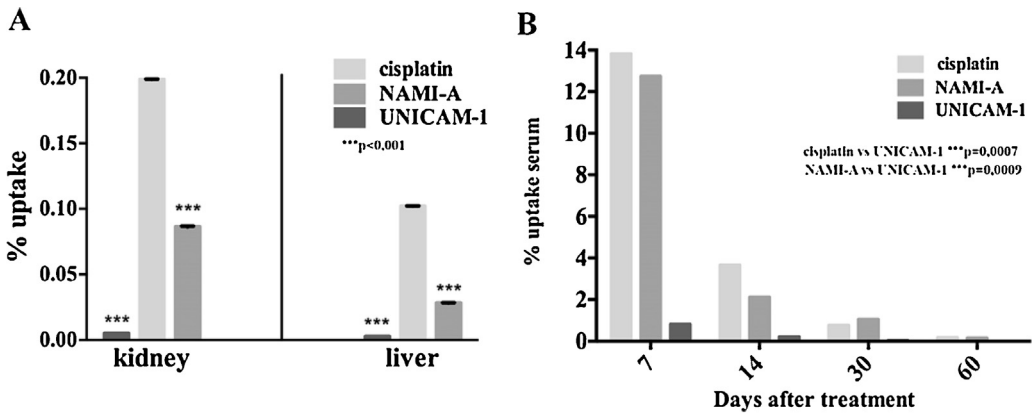

Fig. 4. Ruthenium and platinum content in liver and kidney (A) and serum (B) from mice injected with UNICAM-1, NAMI-A or cisplatin evaluated by Inductively Coupled Plasma-Mass Spectrometry (ICP-MS). The data are presented as% injected dose per gram of tissue (% ID per g). Values are mean ± SEM, n = 10. *p < 0.05; **p < 0.01; ***p < 0.001; ****p < 0.0001 was calculated with an unpaired two-tailed *t*-test. Each group was compared to control.

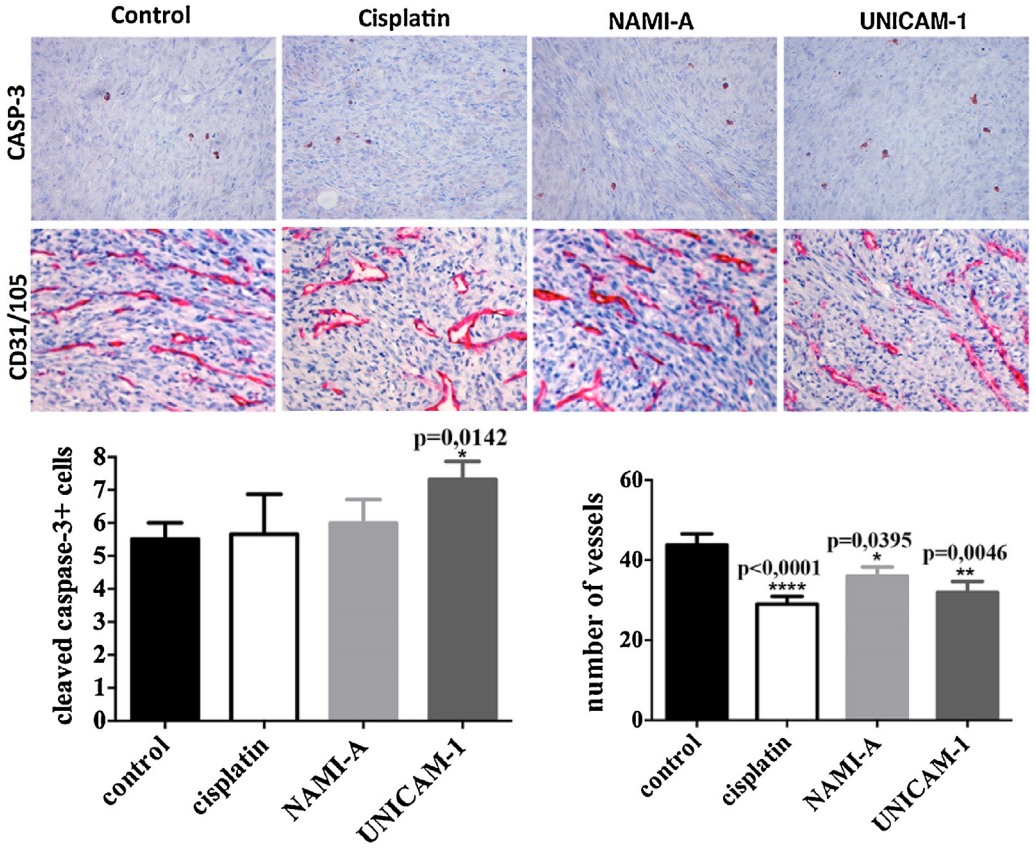

Fig. 5. Analysis of apoptotic cells and vessel number in A17 tumors. Representative images of cleaved caspase-3 and CD31/105 positive immunohistochemical sections of control, cisplatin, NAMI-A and UNICAM-1 treated tumors on day 36 (upper panel). Quantification of cleaved caspase-3 positive cells and number of vessels in control and treated tumors was determined as described in the experimental section (lower panel). Results are represented as means ± SEM from 5 × 400 microscopic fields per tumor (n = 10). *p < 0.05; **p < 0.01; ***p < 0.001; ****p<0.0001 was calculated with an unpaired two-tailed *t* test. Each group was compared to control.

cells in several ways, for example, by depletion of immunosuppressive cells from the tumor bed [38], or through direct effects on malignant cells that then elevate their immunogenicity and their susceptibility to immune control by cytotoxic T and natural killer (NK) cells. Certain chemotherapeutics enhance tumor immunogenicity because they induce a form of apoptosis in cancer cells, known as "immunogenic cell death", that favors the transfer of tumor antigens to dendritic cells (DC), which ultimately "cross-prime" and activate anti-tumorigenic CD4+/CD8+ T-cell immunity. Accordingly, numerous studies have reported a link between response to conventional therapies, and tumor immune infiltrate in several different solid tumor types, including breast cancer [39]. Immunohistochemical analysis of tumors explanted from mice treated with cisplatin, NAMI-A and UNICAM-1 revealed a significantly higher level of tumor immune infiltrates in comparison with control mice (Fig. 6). Our results are concordant with a recent study by Denkert et al. [40], showing that tumor infiltrating lymphocyte levels correlate positively with patient survival and predict pathologic complete response to chemotherapy in human TNBC. In fact, the presence of tumor-infiltrating T lympho-

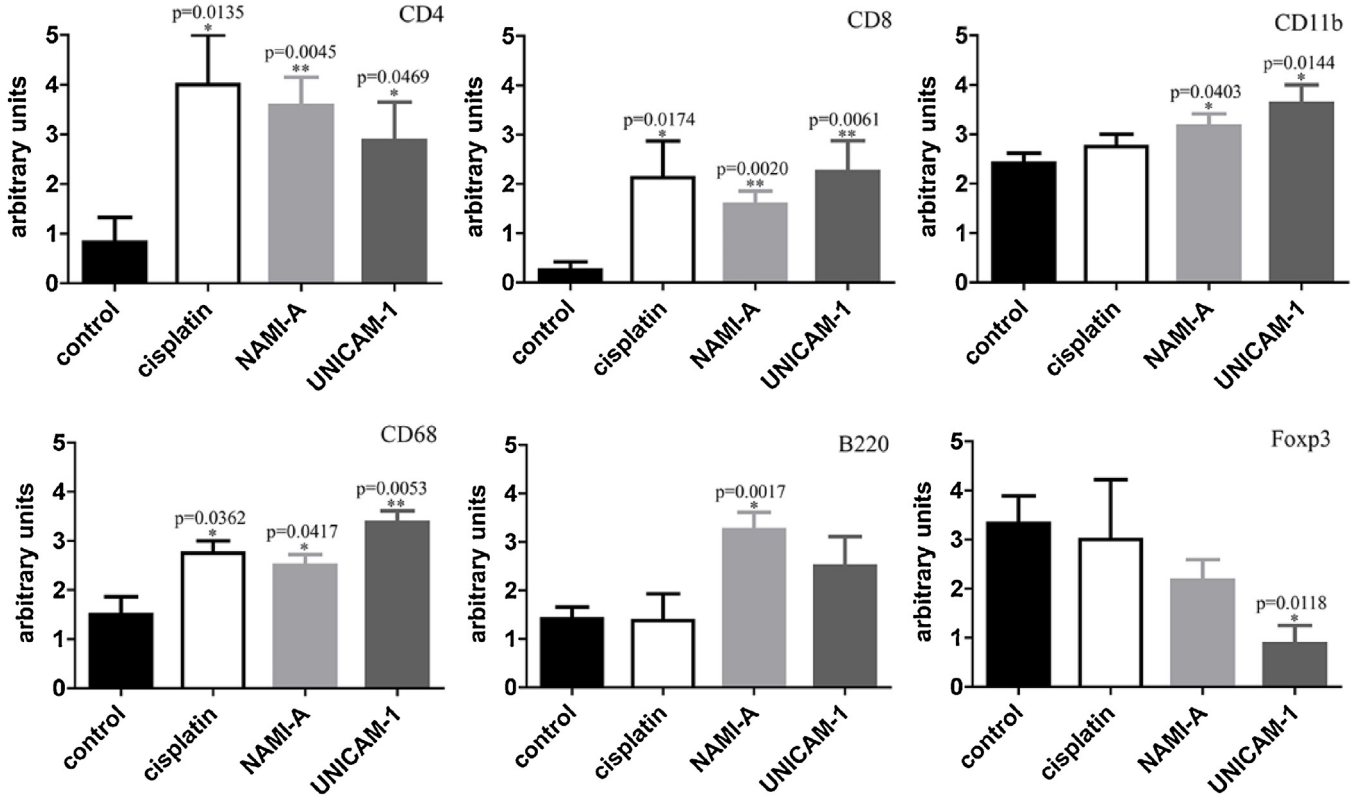

Fig. 6. Semiquantitative analysis of inflammatory infiltration in A17 tumors from control, cisplatin, NAMI-A and UNICAM-1 treated mice (protocol q3 × 4). Data were analyzed as described in the experimental section. Results are represented as means ± SEM from 5 × 400 microscopic fields per tumor (n = 5). CD4+ cells: T-helper lymphocytes; CD8+ cells: cytotoxic-T lymphocytes; CD11b+ cells: dendritic cells; CD68+ cells: macrophages; B220+ cells: B lymphocytes; Foxp3 cells: regulatory T lymphocytes. $^{*}p < 0.05$; $^{**}p < 0.01$; $^{***}p < 0.001$; $^{****}p < 0.0001$ was calculated with an unpaired two-tailed *t* test. Each group was compared to control.

cytes indicates the host immune response to tumor antigens and is considered as a positive marker of response to chemotherapy. However, human tumors also promote accumulation of CD4 + CD25+ immunosuppressive regulatory T cells (Treg, Foxp3 positive cells) in the tumor bed or in the blood. These cells are known as the key contributor to maintenance of immune tolerance [41]. Emerging evidence suggests that Treg cells have an important immunopathologic role in human tumor growth by suppressing endogenous tumor-associated antigen-specific T-cell immunity [42,43]. Tregs can suppress proliferation of activated effector T cells by direct contact, inhibiting their clonal expansion [44], or can induce direct killing of effector cells through release of granzyme and perforin [45,46]. Transforming growth factor-b (TGF-b) and IL-10 secreted by Tregs have also been involved in inhibition of tumor-specific CTL cytotoxicity *in vivo* [47]. Interestingly, following UNICAM-1 treatment the levels of CD4+ and cytotoxic CD8+ T lymphocytes were increased, concomitantly with a strong reduction of Foxp3 regulatory T-cell infiltration (Fig. 6, Supplementary Figs. 4,5). Recently, an immunologic signature consisting of the absence of Foxp3 cells and the presence of a high number of CD8 T cells on final surgical biopsy of breast tumor treated by neoadjuvant chemotherapy has been associated with pathologic complete responses [38,48]. A high CD8/Treg ratio has been also associated with favorable prognosis in epithelial ovarian cancer [49]. However, although induction and expansion of Tregs in the tumor microenvironment are considered critical steps in evasion of the immune response and tumor cell survival, the molecular mechanisms underlying Treg cells recruitment in the primary tumor remain unclear. Clinical studies of breast cancer patients have shown a correlation between increased COX2 expression with high Treg recruitment [50] and recently Karavitis et al. provided direct evidence that COX2, and subsequent PGE2 overexpression, results in a tumor environment that promotes Treg recruitment and attenuation of the normal immune response [51]. COX2 is associated with a basal-like transcription pattern in human breast tumors [34] and it was found significantly overexpressed in A17 tumors, where it correlates with their mesenchymal signature [29,34,35,52,53]. Beside its immunosuppressive effect, COX2 expression has been also linked to cancer progression due to its ability to promote cell proliferation and angiogenesis [36]. We therefore evaluated if there is a correlation between COX2 levels and Treg recruitment in A17 tumors explanted from control and treated animals. Of note, western blot analyses revealed a significant reduction of COX2 expression upon UNICAM-1 treatment (Fig. 7), supporting the association between COX2 levels and Treg infiltration and unraveling the molecular mechanism which might mediate the antitumoral and immunomodulatory action of this ruthenium compound. In addition, UNICAM-1 induces an enhancement of recruitment and infiltration into tumors of cells expressing the dendritic marker CD11b and the macrophage marker CD68 (Fig. 6). Although the role of tumor associated macrophages is still controversial, tumor-infiltrating macrophages often participate in the host response toward the tumor, killing tumor cells [54,55]. In agreement with this finding, high macrophage infiltration has been correlated to improved survival in colorectal cancer [56]. Overall, we report that UNICAM-1 has a relevant therapeutic efficacy against TNBC and its unique immunomodulatory action might explain the observed anticancer effects.

4. Conclusion

Cancer remains a major cause of mortality worldwide. Chemotherapy is one of the most potent strategies to treat tumors,

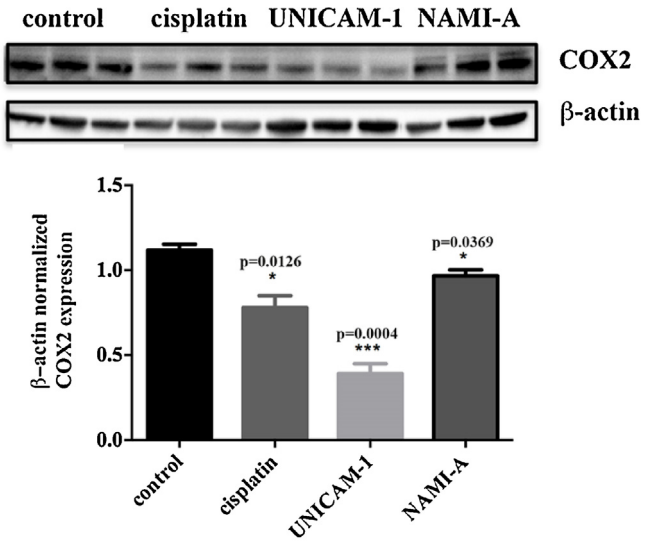

Fig. 7. UNICAM-1 targeted COX2 expression in A17 transplanted tumors. Western blot analysis for the expression levels of COX2 and β-actin (loading control) in A17 tumors from FVB mice receiving isotonic solution (control), cisplatin, UNICAM-1, or NAMI-A (upper panel). Densitometric quantification of COX2 expression normalized on β-actin was performed with ImageJ Software (lower panel). Statistical analysis was executed with GraphPad Prism Software (San Diego, CA, USA), using $p < 0.05$ as the critical level of significance (****$p < 0.0001$; ***$p < 0.001$).

however the toxicity of currently available anticancer drugs represents one of the most critical issues. New therapies, characterized by high efficiency and low toxicity, are therefore an urgent unmet medical need. Conventional cancer therapies, such as chemotherapies, have been developed based on the concept that cancer constitutes a cell-autonomous genetic or epigenetic disease. As a consequence, their cytostatic and/or cytotoxic effects have been tested *in vitro*, on cultured human tumor cells, and on human cancer xenografts growing in immunodeficient mice. Little attention has been given to the host immune system in terms of prognosis and potential response to therapy [57]. On the other hand, the role of the immune system in cancer has long been known and accumulating evidence indicates that the therapeutic efficacy of several antineoplastic agents relies on their capacity to influence the tumor-host interaction and to favorably modify the immune microenvironment.

Our studies were focused on the development and validation of an organometallic ruthenium(II)-arene complex, we called UNICAM-1, as novel anticancer drug. Overall, UNICAM-1 exhibits a marked anti-tumoral activity *in vivo* against an experimental TNBC model, associated with low toxicity and favorable clearance properties. Therapeutic efficacy of UNICAM-1 seems to rely on its capacity to influence the tumor-host interaction, leading to activation of an immune response specific for malignant cells, supporting the hypothesis that chemotherapy is efficient if it succeeds in eliciting anticancer immunosurveillance [37].

Acknowledgments

This study was supported by A. Amici's F.A.R. 2015 of the University of Camerino.

Appendix A. Supplementary data

Supplementary data associated with this article can be found, in the online version, at http://dx.doi.org/10.1016/j.phrs.2016.03.032.

References

[1] T.O. Nielsen, F.D. Hsu, K. Jensen, M. Cheang, G. Karaca, Z. Hu, T. Hernandez-Boussard, C. Livasy, D. Cowan, L. Dressler, L.A. Akslen, J. Ragaz, A.M. Gown, C.B. Gilks, M. van de Rijn, C.M. Perou, Immunohistochemical and clinical characterization of the basal-like subtype of invasive breast carcinoma, Clin. Cancer Res. 10 (2004) 5367–5374.
[2] M.C. Cheang, D. Voduc, C. Bajdik, S. Leung, S. McKinney, S.K. Chia, C.M. Perou, T.O. Nielsen, Basal-like breast cancer defined by five biomarkers has superior prognostic value than triple-negative phenotype, Clin. Cancer Res. 14 (2008) 1368–1376.
[3] F. Bertucci, P. Finetti, D. Birnbaum, Basal breast cancer: a complex and deadly molecular subtype, Curr. Mol. Med. 12 (2012) 96–110.
[4] W.D. Foulkes, I.E. Smith, J.S. Reis-Filho, Triple-negative breast cancer, N. Engl. J. Med. 363 (20) (2010) 1938–1948.
[5] L. Kelland, The resurgence of platinum-based cancer chemotherapy, Nat. Rev. Cancer 7 (2007) 573–584.
[6] M.J. Piccart, H. Lamb, J.B. Vermorken, Current and future potential roles of the platinum drugs in the treatment of ovarian cancer, Ann. Oncol. 12 (2001) 1195–1203.
[7] M. Tian, Y. Zhong, F. Zhou, C. Xie, Y. Zhou, Z. Liao, Platinum-based therapy for triple-negative breast cancer treatment: a meta-analysis, Mol. Clin. Oncol. 3 (2015) 720–724.
[8] D.P. Silver, A.L. Richardson, A.C. Eklund, Z.C. Wang, Z. Szallasi, Q. Li, N. Juul, C.O. Leong, D. Calogrias, A. Buraimoh, A. Fatima, R.S. Gelman, P.D. Ryan, N.M. Tung, A. De Nicolo, S. Ganesan, A. Miron, C. Colin, D.C. Sgroi, L.W. Ellisen, E.P. Winer, J.E. Garber, Efficacy of neoadjuvant cisplatin in triple-negative breast cancer, J. Clin. Oncol. 28 (2010) 1145–1153.
[9] N.J. Wheate, S. Walker, G.E. Craig, R. Oun, The status of platinum anticancer drugs in the clinic and in clinical trials, Dalton Trans. 39 (2010) 8113–8127.
[10] F. Muggia, BRCA-deficient animal models and cisplatin resistance, Gynecol. Oncol. 112 (2009) 275–281.
[11] J. Liu, X. Chen, T. Ward, M. Pegram, K. Shen, Combined niclosamide with cisplatin inhibits epithelial-mesenchymal transition and tumor growth in cisplatin-resistant triple-negative breast cancer, Tumour Biol. (2016) 1–11.
[12] L. Kelland, Ruthenium antimetastatic agents, Nat. Rev. Cancer 7 (2007) 573–584.
[13] N.P. Barry, P.J. Sadler, Exploration of the medical periodic table: towards new targets, Chem. Commun. 49 (2013) 5106–5131.
[14] A.L. Noffke, A. Habtemariam, M.A. Pizarro, P.J. Sadler, Designing organometallic compounds for catalysis and therapy, Chem. Commun. 48 (2012) 5219–5246.
[15] G. Gasser, I. Ott, N. Metzler-Nolte, Organometallic anticancer compounds, J. Med. Chem. 54 (2011) 3–25.
[16] G.S. Smith, B. Therrien, Targeted and multifunctional arene ruthenium chemotherapeutics, Dalton Trans. 40 (2011) 10793–10800.
[17] G. Sava, A. Bergamo, P.J. Dyson, Metal-based antitumour drugs in the post-genomic era: what comes next? Dalton Trans. 40 (2011) 9069–9075.
[18] A.F. Peacock, P.J. Sadler, Medicinal organometallic chemistry: designing metal arene complexes as anticancer agents, Chem. Asian J. 3 (2008) 1890–1899.
[19] E. Alessio, G. Mestroni, A. Bergamo, G. Sava, Ruthenium anticancer drugs, Curr. Top. Med. Chem. 4 (2004) 1525–1535.
[20] R. Trondl, P. Heffeter, C.R. Kowol, M.A. Jakupec, W. Berger, B.K. Keppler, NKP-1339, the first ruthenium-based anticancer drug on the edge to clinical application, Chem. Sci. 5 (2014) 2925–2932.
[21] B. Lippert, Z. Cisplat, Chemistry biochemistry of a leading anticancer drug. The mechanism of action of cisplatin: from adducts to apoptosis, 4, 111–134. Ed.; Verlag Helvetica Chimica Acta: Zurich; Wiley-VCH: Weinheim, Germany (1999).
[22] Z. Adhireksan, G.E. Davey, P. Campomanes, M. Groessl, C.M. Clavel, H. Yu, A.A. Nazarov, H.F. Yeo, W.H. Ang, P. Droge, U. Rothlisberger, P.J. Dyson, C.A. Davey, Ligand substitutions between ruthenium-cymene compounds can control protein versus DNA targeting and anticancer activity, Nat. Commun. 5 (2014) 3462.
[23] A. Casini, C.G. Hartinger, A.A. Nazarov, P.J. Dyson, Organometallic antitumour agents with alternative modes of action, Top. Organomet. Chem. 32 (2010) 57–80.
[24] R.E. Aird, J. Cummings, A.A. Ritchie, M. Muir, R.E. Morris, H. Chen, P.J. Sadler, D.I. Jodrell, *In vitro* and *in vivo* activity and cross resistance profiles of novel ruthenium(II) organometallic arene complexes in human ovarian cancer, Br. J. Cancer 86 (2002) 1652–1657.
[25] C. Scolaro, A. Bergamo, L. Brescacin, R. Delfino, M. Cocchietto, G. Laurenczy, T.J. Geldbach, G. Sava, P.J. Dyson, *In vitro* and *in vivo* evaluation of ruthenium(II)-arene PTA complexes, J. Med. Chem. 48 (2005) 4161–4171.
[26] F. Marchetti, C. Pettinari, R. Pettinari, A. Cerquetella, C. Di Nicola, A. Macchioni, D. Zuccaccia, M. Monari, F. Piccinelli, Synthesis and intramolecular and interionic structural characterization of half-sandwich (arene)ruthenium(II) derivatives of bis(pyrazolyl)alkanes, Inorg. Chem. 47 (2008) 11593–11603.
[27] G. Mestroni, E. Alessio, G. Sava, PCT Int. Appl.WO 98 000431 1998.
[28] M. Galiè, C. Sorrentino, M. Montani, L. Micossi, E. Di Carlo, T. D'Antuono, L. Calderan, P. Marzola, D. Benati, F. Merigo, F. Orlando, A. Smorlesi, C. Marchini, A. Amici, A. Sbarbati, Mammary carcinoma provides highly tumourigenic and invasive reactive stromal cells, Carcinogenesis 26 (2005) 1868–1878.
[29] M. Galiè, G. Konstantinidou, D. Peroni, I. Scambi, C. Marchini, V. Lisi, M. Krampera, P. Magnani, F. Merigo, M. Montani, F. Boschi, P. Marzola, R. Orrù, P. Farace, A. Sbarbati, A. Amici, Mesenchymal stem cells share molecular

signature with mesenchymal tumor cells and favor early tumor growth in syngeneic mice, Oncogene 27 (2008) 2542–2551.
[30] K.G. Daniel, D. Chen, S. Orlu, Q.C. Cui, F.R. Miller, Q.P. Dou, Clioquinol and pyrrolidine dithiocarbamate complex with copper to form proteasome inhibitors and apoptosis inducers in human breast cancer cells, Breast Cancer Res. 7 (2005) 897–908.
[31] R. Gagliardi, G. Sava, S. Pacor, G. Mestroni, E. Alessio, Antimetastatic action and toxicity on healthy tissues of Na[trans-ruCl4(DMSO)Im] in the mouse, Clin. Exp. Metastasis 12 (1994) 93–100.
[32] R.J. Dinis-Oliveira, J.A. Duarte, F. Remião, A. Sánchez-Navarro, M.L. Bastos, F. Carvalho, Single high dose dexamethasone treatment decreases the pathological score and increases the survival rate of paraquat-intoxicated rats, Toxicology 227 (2006) 73–85.
[33] F. Fantuz, S. Ferraro, L. Todini, P. Mariani, R. Piloni, E. Salimei, Essential trace elements in milk and blood serum of lactating donkeys as affected by lactation stage and dietary supplementation with trace elements, Animal 7 (2013) 1893–1899.
[34] C. Marchini, M. Montani, G. Konstantinidou, R. Orrù, S. Mannucci, G. Ramadori, F. Gabrielli, A. Baruzzi, G. Berton, F. Merigo, S. Fin, M. Iezzi, B. Bisaro, A. Sbarbati, M. Zerani, M. Galiè, A. Amici, Mesenchymal/stromal gene expression signature relates to basal-like breast cancers, identifies bone metastasis and predicts resistance to therapies, PLoS One 5 (2010) e14131.
[35] B. Bisaro, M. Montani, G. Konstantinidou, C. Marchini, L. Pietrella, M. Iezzi, M. Galiè, F. Orso, A. Camporeale, S.M. Colombo, P. Di Stefano, G. Tornillo, M.P. Camacho-Leal, E. Turco, D. Taverna, S. Cabodi, A. Amici, P. Defilippi, p130Cas/Cyclooxygenase-2 axis in the control of mesenchymal plasticity of breast cancer cells, Breast Cancer Res. 14 (2012) R137.
[36] G. Singh-Ranger, M. Salhab, K. Mokbel, The role of cyclooxygenase-2 in breast cancer: review, Breast Cancer Res. Treat. 109 (2008) 189–198.
[37] L. Zitvogel, L. Galluzzi, M.J. Smyth, G. Kroemer, Mechanism of action of conventional and targeted anticancer therapies: reinstating immunosurveillance, Immunity 39 (2013) 74–88.
[38] S. Ladoire, L. Arnould, L. Apetoh, B. Coudert, F. Martin, B. Chauffert, P. Fumoleau, F. Ghiringhelli, Pathologic complete response to neoadjuvant chemotherapy of breast carcinoma is associated with the disappearance of tumor-infiltrating foxp3+ regulatory T cells, Clin. Cancer Res. 14 (2008) 2413–2420.
[39] S. Demaria, M.D. Volm, R.L. Shapiro, H.T. Yee, R. Oratz, S.C. Formenti, F. Muggia, W.F. Symmans, Development of tumor-infiltrating lymphocytes in breast cancer after neoadjuvant paclitaxel chemotherapy, Clin. Cancer Res. 7 (2001) 3025–3030.
[40] C. Denkert, G. von Minckwitz, J.C. Brase, B.V. Sinn, S. Gade, R. Kronenwett, B.M. Pfitzner, C. Salat, S. Loi, W.D. Schmitt, C. Schem, K. Fisch, S. Darb-Esfahani, K. Mehta, C. Sotiriou, S. Wienert, P. Klare, F. André, F. Klauschen, J.U. Blohmer, K. Krappmann, M. Schmidt, H. Tesch, S. Kümmel, P. Sinn, C. Jackisch, M. Dietel, T. Reimer, M. Untch, S. Loibl, Tumor-infiltrating lymphocytes and response to neoadjuvant chemotherapy with or without carboplatin in human epidermal growth factor receptor 2-positive and triple-negative primary breast cancers, J. Clin. Oncol. 33 (2015) 983–991.
[41] S. Sakaguchi, M. Ono, R. Setoguchi, H. Yagi, S. Hori, Z. Fehervari, J. Shimizu, T. Takahashi, T. Nomura, Foxp3+ CD25+ CD4+ natural regulatory T cells in dominant self-tolerance and autoimmune disease, Immunol. Rev. 212 (2006) 8–27.
[42] T.J. Curiel, G. Coukos, L. Zou, X. Alvarez, P. Cheng, P. Mottram, M. Evdemon-Hogan, J.R. Conejo-Garcia, L. Zhang, M. Burow, Y. Zhu, S. Wei, I. Kryczek, B. Daniel, A. Gordon, L. Myers, A. Lackner, M.L. Disis, K.L. Knutson, L. Chen, W. Zou, Specific recruitment of regulatory T cells in ovarian carcinoma fosters immune privilege and predicts reduced survival, Nat. Med. 10 (2004) 942–949.
[43] G.J. Bates, S.B. Fox, C. Han, R.D. Leek, J.F. Garcia, A.L. Harris, A.H. Banham, Quantification of regulatory T cells enables the identification of high-risk breast cancer patients and those at risk of late relapse, J. Clin. Oncol. 24 (2006) 5373–5380.
[44] A.M. Thornton, E.M. Shevach, CD4+ CD25+ immunoregulatory T cells suppress polyclonal T cell activation *in vitro* by inhibiting interleukin 2 production, J. Exp. Med. 188 (1998) 287–296.
[45] W.J. Grossman, J.W. Verbsky, W. Barchet, M. Colonna, J.P. Atkinson, T.J. Ley, Human T regulatory cells can use the perforin pathway to cause autologous target cell death, Immunity 21 (2004) 589–601.
[46] W.J. Grossman, J.W. Verbsky, B.L. Tollefsen, C. Kemper, J.P. Atkinson, T.J. Ley, Differential expression of granzymes A and B in human cytotoxic lymphocyte subsets and T regulatory cells, Blood 104 (2004) 2840–2848.
[47] M.L. Chen, M.J. Pittet, L. Gorelik, R.A. Flavell, R. Weissleder, H. von Boehmer, K. Khazaie, Regulatory T cells suppress tumor-specific CD8 T cell cytotoxicity through TGF-beta signals in vivo, Proc. Natl. Acad. Sci. U. S. A. 102 (2005) 419–424.
[48] L. Senovilla, I. Vitale, I. Martins, M. Tailler, C. Pailleret, M. Michaud, L. Galluzzi, S. Adjemian, O. Kepp, M. Niso-Santano, S. Shen, G. Mariño, A. Criollo, A. Boilève, B. Job, S. Ladoire, F. Ghiringhelli, A. Sistigu, T. Yamazaki, S. Rello-Varona, C. Locher, V. Poirier-Colame, M. Talbot, A. Valent, F. Berardinelli, A. Antoccia, F. Ciccosanti, G.M. Fimia, M. Piacentini, A. Fueyo, N.L. Messina, M. Li, C.J. Chan, V. Sigl, G. Pourcher, C. Ruckenstuhl, D. Carmona-Gutierrez, V. Lazar, J.M. Penninger, F. Madeo, C. López-Otín, M.J. Smyth, L. Zitvogel, M. Castedo, G. Kroemer, An immunosurveillance mechanism controls cancer cell ploidy, Science 337 (2012) 1678–1684.
[49] E. Sato, S.H. Olson, J. Ahn, B. Bundy, H. Nishikawa, F. Qian, A.A. Jungbluth, D. Frosina, S. Gnjatic, C. Ambrosone, J. Kepner, T. Odunsi, G. Ritter, S. Lele, Y.T. Chen, H. Ohtani, L.J. Old, K. Odunsi, Intraepithelial CD8+ tumor-infiltrating lymphocytes and a high CD8+/regulatory T cell ratio are associated with favorable prognosis in ovarian cancer, Proc. Natl. Acad. Sci. U. S. A. 102 (2005) 18538–18543.
[50] B.A. Pockaj, G.D. Basu, L.B. Pathangey, R.J. Gray, J.L. Hernandez, S.J. Gendler, P. Mukherjee, Reduced T-cell and dendritic cell function is related to cyclooxygenase-2 overexpression and prostaglandin E2 secretion in patients with breast cancer, Ann. Surg. Oncol. 11 (2004) 328–339.
[51] J. Karavitis, L.M. Hix, Y.H. Shi, R.F. Schultz, K. Khazaie, M. Zhang, Regulation of COX2 expression in mouse mammary tumor cells controls bone metastasis and PGE2-induction of regulatory T cell migration, PLoS One 7 (9) (2012) e46342.
[52] C. Garulli, C. Kalogris, L. Pietrella, C. Bartolacci, C. Andreani, M. Falconi, C. Marchini, C. Amici, Dorsomorphin reverses the mesenchymal phenotype of breast cancer initiating cells by inhibition of bone morphogenetic protein signaling, Cell. Signal. 26 (2014) 352–362.
[53] C. Kalogris, C. Garulli, L. Pietrella, V. Gambini, S. Pucciarelli, C. Lucci, M. Tilio, M.E. Zabaleta, C. Bartolacci, C. Andreani, M. Giangrossi, M. Iezzi, B. Belletti, C. Marchini, A. Amici, Sanguinarine suppresses basal-like breast cancer growth through dihydrofolate reductase inhibition, Biochem. Pharmacol. 90 (3) (2014) 226–234, http://dx.doi.org/10.1016/j.bcp.2014.05.014.
[54] S. Cui, J.S. Reichner, R.B. Mateo, J.E. Albina, Activated murine macrophages induce apoptosis in tumor cells through nitric oxide-dependent or -independent mechanisms, Cancer Res. 54 (1994) 2462–2467.
[55] J.H. Martin, S.W. Edwards, Changes in mechanisms of monocyte/macrophage-mediated cytotoxicity during culture Reactive oxygen intermediates are involved in monocyte-mediated cytotoxicity, whereas reactive nitrogen intermediates are employed by macrophages in tumor cell killing, J. Immunol. 150 (1993) 3478–3486.
[56] J. Forssell, A. Oberg, M.L. Henriksson, R. Stenling, A. Jung, R. Palmqvist, High macrophage infiltration along the tumor front correlates with improved survival in colon cancer, Clin. Cancer Res. 13 (2007) 1472–1479.
[57] C. Jochems, J. Schlom, Tumor-infiltrating immune cells and prognosis: the potential link between conventional cancer therapy and immunity, Exp. Biol. Med. 236 (2011) 567–579.